

Modularizing and Validating CFD Parts of Four-way Cassette Type Outlets

Hidekazu Tanaka¹, Masashi Imano¹, Yuzo Sakamoto¹

¹ Affiliation, the University of Tokyo, Dept. of Architecture, Tokyo, Japan 113-8656

Abstract:

In this paper, we created the CFD parts of four-way cassette type outlets for predicting easily the thermal environment of an office with packaged unit air-conditioning systems. At first we measured detail distributions of wind velocity around the cassette type outlets in two cases of angles of flap in an experiment room with particle image velocimetry (PIV).

Secondly we created the CFD parts of this type of outlets and performed CFD analysis. As a result of examining the correlation with measured velocity distribution around the outlets, we have confirmed the validity of these CFD parts.

Keywords: CFD, AC unit, PIV

1. Introduction

We created the CFD parts of a four-way cassette type outlet which is the most popular air

conditioning as the internal terminal. The supply-air is one of the important factors of constructing the thermal environment therefore the simulating model which can reproduce the airflow such as the distance of reaching and the way of diffusing is needed. In order to create such a model, we need the minute visualization and measurement of the supply-air.

We used the PIV for measuring the minute distribution of average velocity of the airflow.

In addition, we checked the characteristics of the turbulence and two-dimensional nature of the wind velocity by using supersonic wind velocimeter. Based on these data, we created the CFD parts of the outlet and analyzed the PIV measuring room with these parts.

2. Measurement of the Supply-Air

2.1. Measurement by PIV

2.1.1. Device and Criteria

The measurement was performed in the two cases of the angle of flaps of a four-way

cassette type outlet, ‘Horizontal’ and ‘Vertical’. Then the velocity of wind was 22.0 m/s,

and considering the symmetry of the shape, only one side of the outlet was measured (the

measurement area is shown in Fig. 1). Pictures of five sections were taken every 50mm

intervals, defining the central section as Section 1. The measuring devices were arranged

like Fig. 2. The outlet was put upside down and a board simulating a ceiling was put for the

convenience of measurement. The source of light was the 120mJ Double Pulse YAG Laser

(produced by DANTEC co., Microwave) and exposed as the sheet light 1mm thick. The

pictures of the measuring area were taken vertically by a CCD camera (produced by

DANTEC co., FlowSenseM2). The vectorial velocity was calculated by Direct Mutual

Correlative Method, and defined the check area as 32 times 32 pixels. 100 pictures were

taken every section and were averaged in order to capture the steady property of airflow.

2.1.2. Result of Measurement

The result of this measurement is shown in Fig. 3 and 4. The angle of the supply-air is

about 30 degrees at 'Horizontal' and about 80 degrees at 'Vertical'. From the center to the

edge in these cases, the angle of supply-air changes vertically. The width of airflow is

almost the same in these cases, and the dependence on the flaps is considered to be small.

2.2. Measurement by Supersonic Wind Velocimeter

2.2.1. Device and Criteria

Since a PIV is two-dimensional, the factor of velocity vertical to the laser sheet can't be

obtained. It seems that the characteristic of supply-air is quite two-dimensional. In order to

check it, a measurement by three-dimensional supersonic wind velocimeter is performed

(produced by KAIJO, Type WA-590). The velocity is measured at the point shown on Fig.5

in the PIV measuring section 1 to 4. The measuring frequency was 200Hz and the number

of measurement on each point was 8008.

2.2.2. Result of Measurement

The results of calculating average wind velocity, turbulence energy, angle from the vertical

plane, turbulence intensity and the scale of the length of a vortex (refer to Eq.1, 2 and 3)

from the measurement are shown in Table 7 and 8 (refer to the Fig. 6 for the direction of the factor of velocity).

$$I = (2/3K)^{0.5} / U \times 100 \quad (\text{Eq.1})$$

$$L_i = U \cdot \sum_j \langle u_i(t) \cdot \Delta t \rangle \cdot u_i(t) / \langle u_i(t)^2 \rangle \quad (\text{Eq.2})$$

$$L = (L_1 + L_2 + L_3) / 3 \text{ when } \Delta t (i=1,2,3)_1 \quad (\text{Eq.3})$$

u, v, w : three-dimensional factor of wind velocity (see Fig.6)

U : scalar wind velocity[m/s] k : turbulence energy[m²/s²] I : turbulence intensity[%]

θ : angle from the vertical plane[deg] L : scale of the length of a vortex[mm]

Δt : interval of measurement[s]

The factor of velocity u , vertical to the laser sheet, is at most 0.5m/s and the declination is

less than 5 to 10 degrees. It is considered that this factor is so small that there is no problem

by ignoring it in creating a model for simulation.

3. Creating CFD Parts

3.1 Creating the Parts of Measurement Data

The parts of measurement data were created in case of average wind velocity, turbulence

intensity and the scale of the length of a vortex from the measurement near the four-way

cassette type outlet, measured in 2.1. The parts consist of external files of STL format

which describe the body of the outlet in XML format, and external files of VTK format

which describe the data of a field of measured average wind velocity, turbulence intensity

and the scale of the length of a vortex. Since we assumed the symmetry of plane and

rotation in PIV measurement and measured in half of one outlet, we extracted the data

according to the symmetry and created the data of a field corresponding to the four outlets.

We show the data of the shape and distribution of velocity is shown in Fig. 9, visualized by

ParaView, an open-source tool for visualization.

3.2. Creating CFD Parts

The CFD parts were created, which inherit the measurement parts based on the external

files of the shape and the external file of the data of a field included in the measurement

parts created in 3.1. Then the serial numbers of the measurement parts were put as the

reference serial number of the CFD parts in order to show the inheritance of the

measurement data. The turbulence energy and the rate of dissipating of the turbulence

energy were included in addition to average wind velocity, turbulence intensity and the

scale of the length of a vortex, which are normally necessary for analyzing by CFD in a

RANS turbulence model. The rate of dissipating of the turbulence energy was calculated

from the turbulence energy and the scale of the length of a vortex by assuming the local

balance of the energy.

4. Analyzing and Validating with CFD Parts

4.1. Criteria for Analyzing by CFD

The case of PIV measurement experiment on 2.1 by CFD was analyzed with the parts

created on 3.2 (the criteria are shown in Table 10). The analyzing area is shown in Fig. 11,

but considering the symmetry of the field of flow, only the 1/4 symmetric area shown in the

figure is analyzed. When practical analysis of the anemostat type outlets and cassette type

outlets by CFD is done, the boundary and criteria of bounds of the AC unit, outlets and

inlets are often modeled. The AC unit as rectangular by BOX Method, a kind of modeling,

was modeled and analyzed¹⁾.

The Table 12 is the cases of calculation for validating the parts, and we validated it by

changing the height of the modeling boundary of this AC unit (the width is fixed) and the

interval of the grids. These parts have three-dimensional distribution of velocity, but the

BOX Method needs the two-dimensional distribution of velocity at the outlets of modeled

boundary. So we interpolated the wind velocity at the outlets of modeled boundary of each

case from three-dimensional distribution of field velocity. Since the volume of wind

changes when interpolating the wind velocity, we scaled the wind velocity at the boundary

in order to adjust the volume of wind to what is described in the parts. We are due to have

the interpolation of the data of the field to the modeled boundary and the process for saving

the plane integration (wind volume for velocity) implemented by CFD vendors as the

function of the parts.

4.2. Validation of the CFD Parts

The correlation (the velocity v and w) between the measured value and the result of CFD

analysis of case 1 with RNG K-Epsilon model is shown in the Fig. 13. The square value

of R of the measured value and the result of CFD analysis in each wind direction and each

case is shown in the Table 14 and 15. The correlation above and on the v side of the PIV

measurement area was checked. The correlation of Standard K-Epsilon model was about

0.027(U), 0.021(w) and 0.037(u) worse than that of RNG K-Epsilon model in average. The

correlation becomes poor (especially in the case of ‘Vertical’) in case 2 which has 2.5mm

lower boundary than case 1. In case 3 in which the interval of grids is 5mm, the correlation is quite poor. The case 1, which has a high modeling boundary and fine interval of grids of 2.5mm, shows a good correlation and we find that we should set the height of modeling boundary and interval of grids to such a level in order to analyze by CFD minutely. The interval of grids could be rough in the area far from the outlet, and further validation in the case of measurement in distant points is needed about the interval of grids and correlation of wind velocity in distant points.

5. Conclusion

The airflow of a four-way cassette type outlet was measured and the steady characteristic was revealed by PIV. The two-dimensional characteristic was checked and the turbulence factor by a supersonic wind velocimeter was measured. The results of the measurement were converted into CFD parts, the measurement room was analyzed by CFD and the parts were validated. We found out that by moderately taking the height of the modeling

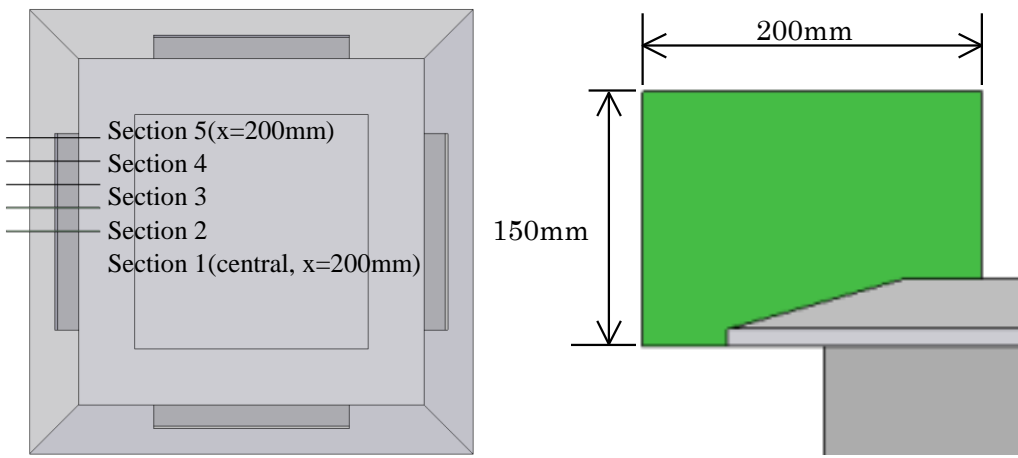
boundary and the interval of grids, we can accurately reproduce the distribution of the wind velocity near the outlet.

[acknowledgement]

This paper was written with the help of the members of CFD parts WG in SHASE(the Society of Heating, Air-Conditioning and Sanitary Engineering of Japan). We appreciate the cooperation to the persons concerned.

[references]

MOMOI Yoshihisa, YAMANAKA Toshio, KOTANI Hisashi et al. “**CFD of Airflows in Rooms with Anemostat Type Air Diffuser : Part 5. CFD Simulation Using Measured Values of Velocity and Turbulence Parameters in Large Space as Boundary Conditions**” pp775～776 : 2001



a) Location of Measuring Section b) Size of Measurement Area

Fig.1 Measurement Area

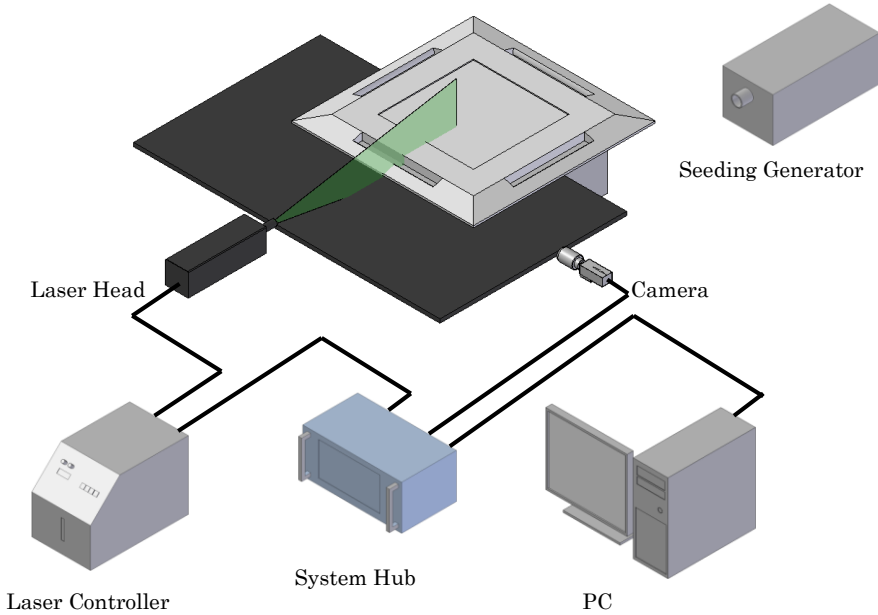
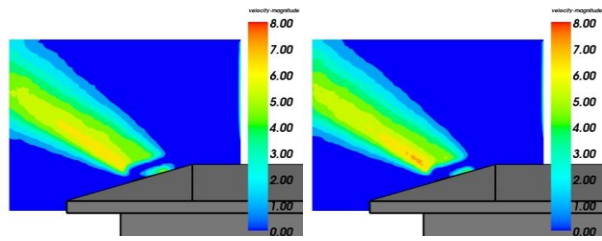
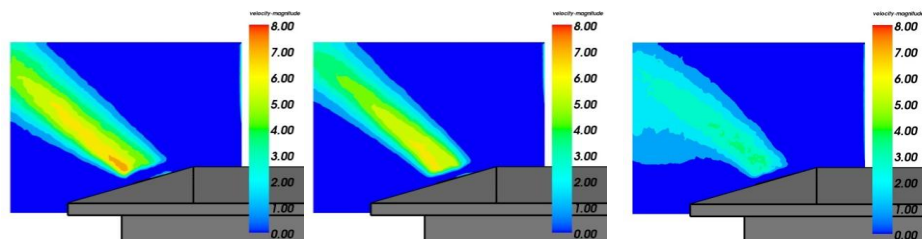


Fig.2 Measuring Devices

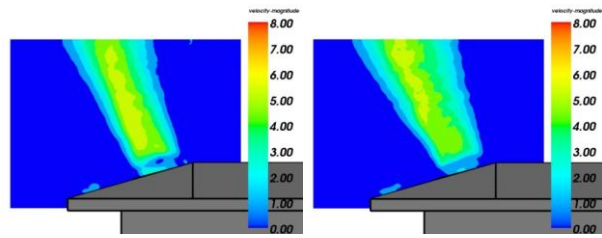


a) Section 1(central, x=0mm) b) Section 2(x=50mm)

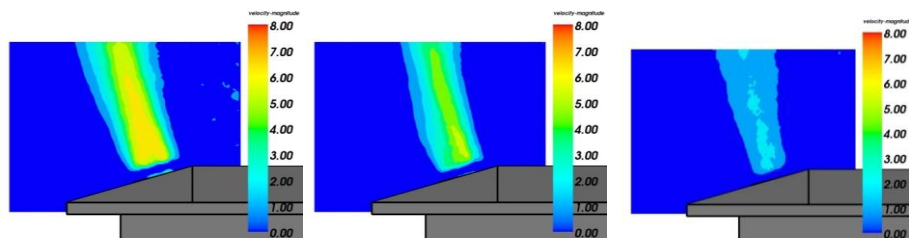


c) Section 3(x=100mm) d) Section 4(x=150mm) e) Section 5(x=200mm)

Fig.3 Distribution of Velocity (Horizontal)



a) Section 1(central, x=0mm) b) Section 2(x=50mm)



c) Section 3(x=100mm) d) Section 4(x=150mm) e) Section 5(x=200mm)

Fig.4 Distribution of Velocity (Vertical)

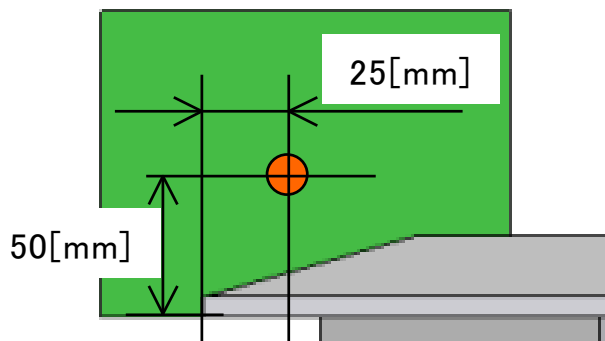


Fig.5 Measuring Point

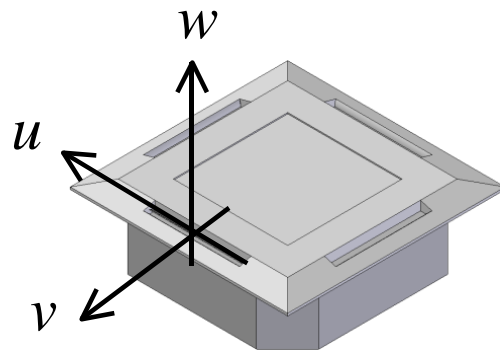


Fig.6 Direction of Factors of Velocity

Table 7 Average Wind Velocity, Factor of Turbulence and Angle from Vertical Section

(Horizontal)

	u [m/s]	v [m/s]	w [m/s]	U [m/s]	k [m ² /s ²]	I [%]	θ [deg]	L [mm]
Section1	0.24	3.21	2.26	3.94	0.11	6.8	3.5	3.6
Section2	0.14	2.44	1.72	2.99	0.12	9.4	2.7	3.1
Section3	0.25	2.55	1.79	3.12	0.13	9.6	4.6	4.1
Section4	0.50	2.36	1.85	3.04	0.18	11.3	5.0	6.0

Table 8 Average Wind Velocity, Factor of Turbulence and Angle from Vertical Section

(Vertical)

	u [m/s]	v [m/s]	w [m/s]	U [m/s]	k [m ² /s ²]	I [%]	θ [deg]	L [mm]
Section1	0.28	1.23	4.58	4.75	0.08	4.9	3.3	3.6
Section2	0.27	1.46	5.41	5.61	0.06	3.6	2.8	3.1
Section3	0.26	0.82	3.73	3.83	0.20	9.5	3.9	4.1
Section4	0.16	0.22	1.25	1.27	0.16	25.7	7.0	6.0

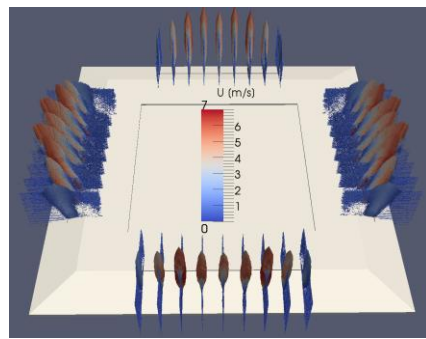


Fig.9 Data of Actual Shape of the Part and Data of Velocity Field

Table 10 Criteria for CFD Analysis

CFD Software	Open Source CFD Tool OpenFOAM
Analyzing Area	1.5m(x) × 1.5m(y) × 1.5m(z)
Width of Grids	2.5cm or 5cm
Solution	SIMPLE(Static Solution)
Turbulence Model	RNG $k-\varepsilon$
Advective Term Scheme	TVD Scheme (limited Upwind)
Boundary Wall	Generalised PowerLaw for Smooth Wall
Criteria for Inlet	Pressure Fixed

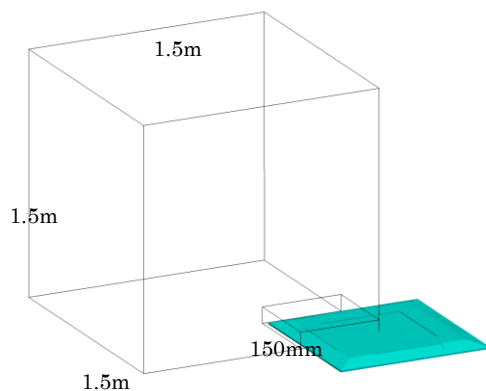


Fig.11 Area of CFD Analysis

Table 12 Cases of CFD Analysis

Case	Height of Model Boundary [cm]	Interval of Grids [cm]
1	10	2.5
2	7.5	"
3	10	5

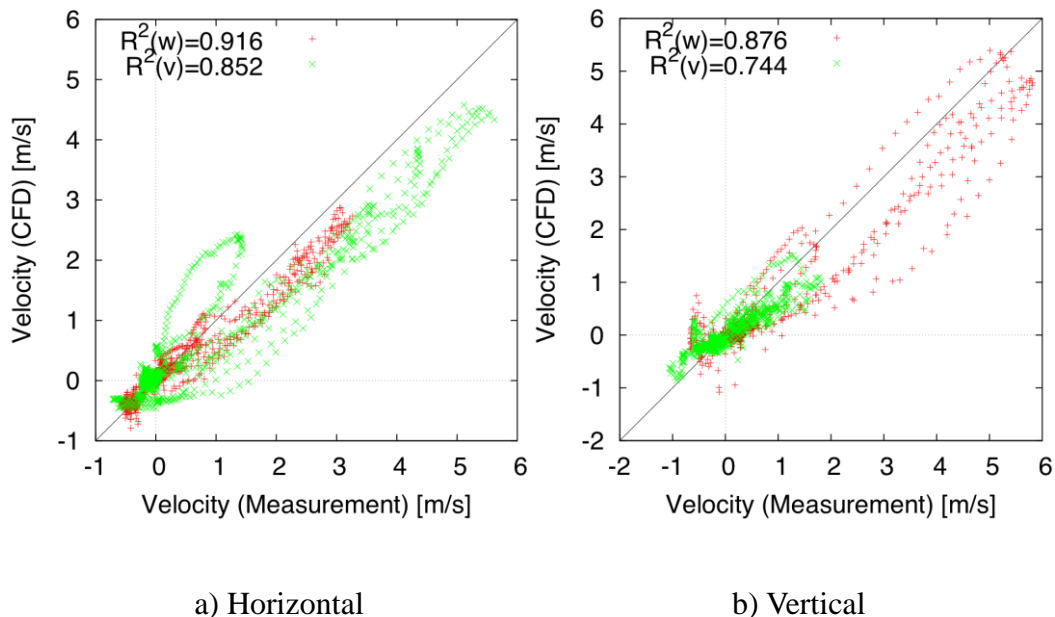


Fig.13 Correlation of Wind Velocity between Measurement and CFD (Case 1, RNG)

Table 14 Square Value of R of Measurement and CFD (Horizontal, RNG)

Case	w (z velocity)	v (y velocity)	U (scaler)
1	0.916	0.852	0.808
2	0.880	0.807	0.747
3	0.702	0.547	0.128

Table 15 Square Value of R of Measurement and CFD (Vertical, RNG)

Case	w (z velocity)	v (y velocity)	U (scaler)
1	0.876	0.744	0.806
2	0.801	0.626	0.714
3	0.648	0.615	0.422